Scanning Electron Microscopy and Differential Scanning Calorimetry Study of the Transition Front in Uniaxially Stretched Isotactic Polypropylene

J. C. RODRÍGUEZ-CABELLO,[1] M. ALONSO,[2] J. C. MERINO,[1] and J. M. PASTOR[1,*]

[1]Dpt. Física de la Materia Condensada, Facultad de Ciencias/E.T.S.I.I., and [2]Dpt. Química Analítica, E.U.P., Universidad de Valladolid, Valladolid, Spain.

SYNOPSIS

This work discusses the potential of calorimetric (DSC) measurements to study the deformation process of semicrystalline polymer samples. It has been pointed out that parameters such as lamellar fragmentation and the parameter of intrachain melting cooperativity suffered significant changes, showing that the stretching process strongly modifies the structure of the isotatic polypropylene (iPP) sample. Furthermore, the observed changes are restricted to a small region between the isotropic and fibrillar regions which is called the transition front. By observing the evolution of the parameter of intrachain melting cooperativity in comparison with lamellar thickness, it has been possible to characterize, at least in a qualitative way, the origin and further evolution of the double-fold molecules; totally extended polymer chain connecting two adjacent crystallites in the fibrillar structure—"tie molecules." Thus, the procedure described here allows, in a simple way, the observation of these molecules, being a possible alternative to TEM methods. Finally, scanning electron microscopy helped in the interpretation of the calorimetric results, revealing that the intermediate values of the different measurements made in this work must be understood as the macroscopic average of the inhomogeneous mixture of the two different structures coexisting in the transition front, i.e., newly formed fibrillar structures and the remains of the original spherulitic structure. © 1996 John Wiley & Sons, Inc.

INTRODUCTION

The deformation behavior and ultimate mechanical properties are very important characteristics of semicrystalline polymers. These properties have been extensively studied and various hypotheses have been presented to explain the observed behavior. In contrast to our detailed comprehension of the deformation of rubberlike substances, an understanding of the molecular mechanism underlying the deformation of semicrystalline polymers has proven to be more complicated. The main reason for the slow progress is crystallinity and complications introduced by the resulting structure and morphology.

For the scope of this work, stretching is considered as a large deformation process for which, starting from an isotropic sample, an oriented material with a high increase of its length is obtained. For semicrystalline polymers, such a phenomenon is the sum of different elastic and plastic deformations. In a cold-drawing process, the mechanism of sample deformation begins with the elastic deformation of the sample (the Hookean zone). After that stage, and according to Peterlin and other authors,[1-23] the structural changes that can take place on a bulk semicrystalline polymer occur in a three-stage process: plastic deformation of the original spherulitic structure, inhomogeneous transformation of the spherulites into the

* To whom correspondence should be addressed.

Journal of Applied Polymer Science, Vol. 60, 1709–1717 (1996)
 CCC 0021-8995/96/101709-09

fiber by micronecking, and the plastic deformation of the fiber structure. The plastic deformation begins in the vicinity of the yield point and marks the birth of the transition front that will delimit the macroscopic neck.

Regarding the phenomena involved in plastic deformation, there is a clear need for contributions from different techniques to advance the formulation of molecular models. First, global measurements such as mechanical properties, light, or X-ray diffraction were employed. Soon these were completed with observations able to discriminate at the microscopic level (mainly, electron microscopy). With the correlation of both kinds of data, different models were established, as the one proposed by Peterlin (see Ref. 11 for a global exposition of experiences and the original formulation of the model). In recent years, others contributions coming from different techniques have been also applied more or less successfully in the refining of the proposed models; those based on spectroscopic methods deserve special mention.[24–30]

However, there is a lack of information coming from calorimetric measurements, especially from differential scanning calorimetry (DSC). This is due to the comparatively short (but dynamic) history of the technique and from the difficulty in extracting structural information, other than crystallinity, from the DSC curves.

This article was devoted to that idea. With the base of different works in which the process of heating and melting and the shape and position of the DSC curve are related to structural parameters, the interphases (transition fronts) between the isotropic and the fibrillar morphology of a uniaxially stretched isotactic polypropylene (iPP) sample was studied. Furthermore, electron microscopy has been used to understand the macroscopic data supplied by the DSC method in terms of observed superstructures.

EXPERIMENTAL

iPP Samples

The iPP used in this work was a commercial polymer designated as PP-051, kindly provided by REPSOL Química S.A. (Madrid, Spain). Its molecular characteristics are M_w = 248 297, M_w/M_n = 6.24, and isotacticity = 97% (from ^{13}C-NMR data).

Plates of the material were prepared by compression molding (Schwanbenthan Polystat 200T hot press) of the received pellets at a temperature of 190°C. The sheets formed in this way were quenched to room temperature. The test specimens were cut from 10 mm-thick plates. Their dimensions were standard for stretching specimens (type III, ASTM D 638-77a test, tensile properties of plastics). The stretching speed was 1 mm/min.

Scanning Electron Microscopy (SEM)

A Jeol-820 scanning electron microscope was used for observation of the iPP samples. The observed sample was a 25 mm-long portion of the deformed sample (see Fig. 1), which included part of the oriented (fibrillar) zone, the transition front, and part of the isotropic zone, the transition front being situated about the center of the selected piece. That piece was cut along the stretching direction parallel to the sample surface, and following the treatment suggested by Aboulfaraj et al.,[31] the inner flat surface was progressively abraded using several different emery papers, polished with alumina powder (0.1 μm), and, finally, chemically etched to reveal its structure.

Differential Scanning Calorimetry Studies

A Mettler (Greinfensee, Switzerland) thermal analysis system was employed for the DSC measure-

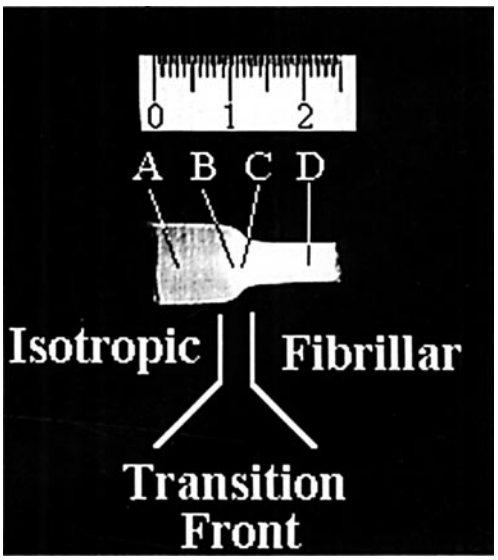

Figure 1 View of the portion of the uniaxially stretched iPP sample studied in this work. The points A, B, C, and D represent an approximate location of the micrograph shown in Figure 2.

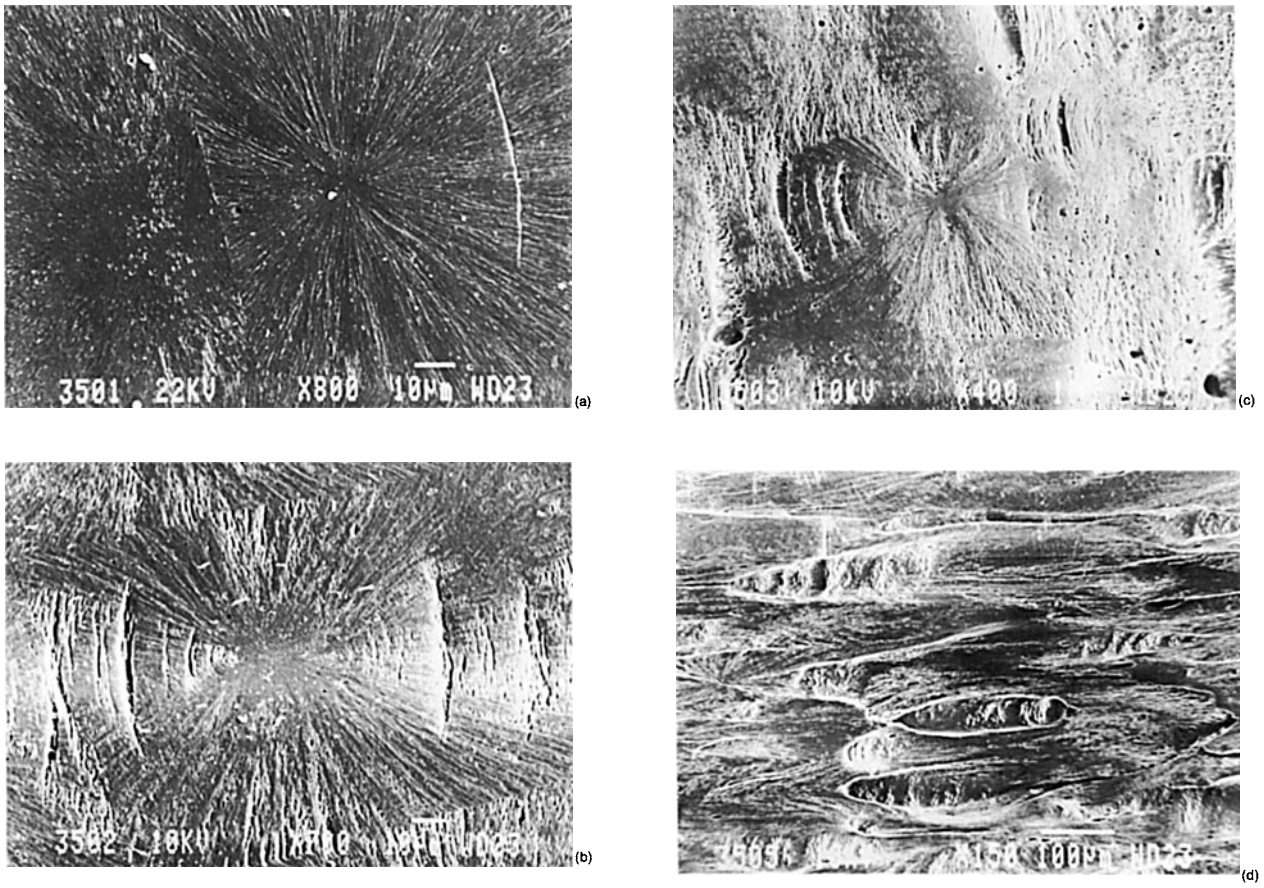

Figure 2 SEM micrographs of the sample. A, B, C, and D, the same as in Figure 1. Stretching direction is on the horizontal.

ments. Small portions weighing about 1.5 mg were used to observe the melting behavior. The DSC conditions were heating from 373 to 473 K at different rates.

RESULTS AND DISCUSSION

The main objective of the present work was the study of the transition front in stretched samples of bulk iPP from the point of view of the calorimetric methods. A picture of the studied zone, in which the transition front is included, can be seen in Figure 1. From the same picture, the magnitude of the transition front can be estimated about 4–5 mm, which is a reasonable extension considering the material used, the stretching speed, and the dimensions of the original sample.

SEM Imaging of the Transition Front

An SEM view of the evolution of the microstructure in the stretched iPP sample can be seen in Figure 2. Figure 2(a) was obtained in a point far away from the transition front and the deformed zone. At that point, the spherulitic nature of the polymer is evident. As the observation point went into the transition front, the spherulitic structure appeared distorted; the spherulite showed ellipsoidal geometry and the presence of cracks [Fig. 2(b)]. The beginning of the plastic deformation of the spherulite coincides with the appearance of the first cracks. That behavior can be explained by the high amount of imperfections of different origins existing in the crystalline regions of bulk samples. The same pattern was observed in all deformed spherulites: arc-shape cracks in the stretching direction and radial cracks in the perpendicular. The shape of these cracks seem to be the result of a compromise between

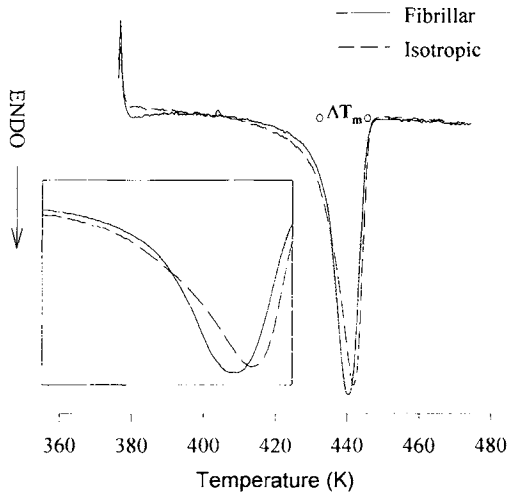

Figure 3 Sample of the thermograms obtained for the studied sample (heating rate 10 K min^{-1}). The continuous line stands for the thermogram of the material in the fibrillar zone, and the dashed line, for the isotropic. On the left corner, a magnification of the melting peak can be seen. Dotted lines show an example of the method used to estimate ΔT_m on the thermogram.

the spherical nature of the original spherulite and the common trend of the materials to form cracks growing perpendicular to the stretching direction.[32,33] Fibrillar structures and voids in the stretching direction, usually known as "crazes," can be distinguished inside the cracks. Going toward the deformed region, the extention of cracks became predominant and the remaining spherulitic structures corresponded to residuals of the cores of the initial spherulites [Fig. 2(c)]. Finally, already in the oriented region, the spherulitic structure has disappeared and only fibrillar structures can be observed [Fig. 2(d)].

Calorimetric Study of the Deformed iPP Sample

Study of the Isotropic and Fibrillar Regions

Samples from the isotropic and fibrillar regions, far from the transition front, were first studied. These samples were subjected to thermal analysis. A sample of the results is shown in Figure 3. In that figure, a magnification around the melting peak is shown for samples from both zones: one in the isotropic and one in the fibrillar. The main differences observed in the thermograms were a displacement of the melting temperature (T_m), which is considered as the temperature at the minimum of the curve, changes in the melting range (ΔT_m), which is calculated as schematically shown in Figure 3 for one of the curves, and changes in the area of the endothermic peak, ΔH_m, which is related to the crystallinity of the material.

Three melting points must be distinguished in the analysis of a polymer, viz:

(i) the experimental T_m obtained for a given heating rate and corresponding to the maximum of the endothermal melting peak;
(ii) the true, physical point T_m^t for a given crystalline structure of the polymer; and
(iii) the equilibrium melting point of a perfect crystal T_m^0.

Usually, T_m^t and T_m do not coincide because the "overheating" of the crystals (important at high rates) and their transformation under the experimental conditions (predominant at low rates). Adequate values of T_m^t can be obtained by extrapolation of the linear sections (at increased rates) of the resulting plot of T_m vs. the square root of the heating rate ($v^{1/2}$) to $v = 0$. This study was made for the isotropic and fibrillar zones of the deformed iPP and their results can be seen in Figure 4. The analysis yields a value of $T_m^t = 429.0$ K for the fibrillar and 431.1 K for the isotropic zone.

The deviation between T_m^t and T_m^0 can be described by a Thomson–Gibbs equation of the form[34]

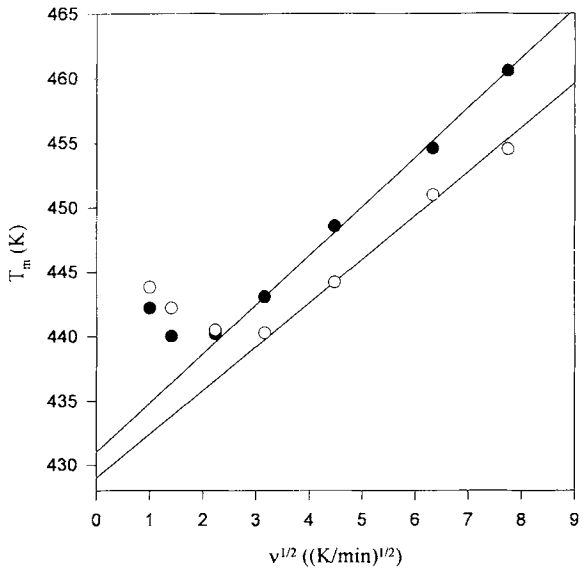

Figure 4 Melting points of (●) isotropic and (○) fibrillar zones of iPP deformed samples vs. heating rate.

$$T_m^t = T_m^0\left(1 - \frac{2\gamma_i}{\Delta H_m^0 \rho_c \lambda_c} - \frac{4\gamma}{\Delta H_m^0 \rho_c \lambda_c'}\right) \quad (1)$$

where γ_i relates to free surface energy of the end faces at which chains fold; γ is the free surface energy of the crystal side surface; ρ_c the density of the crystal; λ_c, the longitudinal dimension of the crystal (lamellar thickness); and λ_c' the lateral dimension.

In an undeformed iPP sample with a spherulitic structure, λ_c' is several orders of magnitude higher than λ_c and, then, eq. (1) becomes

$$T_m^t \approx T_m^0\left(1 - \frac{2\gamma_i}{\Delta H_m^0 \rho_c \lambda_c}\right) \quad (2)$$

This expression can be used to obtain values of λ_c when the parameters T_m^t, T_m^0, ΔH_m^0, and γ_i are known. The values of $\gamma = 11.5 \cdot 10^{-7}$ J cm^{-2}, $\gamma_i = 102 \cdot 10^{-7}$ J cm^{-2}, $\Delta H_m^0 = 196$ J/cm^3, and $T_m^0 = 464$ K were previously published elsewhere.[35] A value of 0.936 g cm^{-3} was adopted for ρ_c according to Ref. 36.

According to eqs. (1) and (2), changes in T_m^t can be associated to changes in the longitudinal dimension, λ_c, of the iPP crystals. However, changes in the lamellar thickness are only possible if the sample melts and recrystallizes during the stretching process. That possibility is covered in some of the plastic deformation models for semicrystalline polymers existing in the bibliography,[16-19] but evidence of such melting has only been found when the temperature of stretching is close to the melting temperature of the polymer and the speed of stretching was high. Our stretching conditions are considerably different from those, so changes in the dimension of chain folding are not plausible for our sample. On the other hand, in deformed iPP samples, lamella fragmentation was proposed in the majority of the standing models of plastic deformation. That breaking will likely yield relatively small crystallites in which, unlike lamellar crystals, the longitudinal (λ_c) and lateral (λ_c') dimensions of the fibrillar crystallites can be of the same order. For this reason, eq. (2) does not hold and eq. (1) must be used to explain the shift in T_m^t.

In the isotropic region, eq. (2) can be used to estimate a value of $\lambda_c = 15.7$ nm, which will not significantly change during the stretching. With the knowledge of all parameters needed and the value of λ_c recently obtained by eq. (2), a values of $\lambda_c' = 54.8$ nm can be estimated by eq. (1) for the fibrillar region.

On the other hand, polymers melt over a temperature range ΔT_m, which sometimes reaches scores of Kelvins. The quantity ΔT_m, which depends on the conditions of polymer crystallization, the annealing conditions, molecular length, polydispersion, and the measurement conditions, is usually related to λ_c in accordance with eq. (1) or (2). However, the actual width of the experimental melting peaks may depend on three factors—a methodological one, the dispersion of l_c, and the parameter of intrachain cooperativity, ν.

The methodological factor due to the thermal lag can be avoided by a similar way to that used for T_m. True values of ΔT_m (ΔT_m^t) extrapolated to $\upsilon = 0$ were obtained (see Fig. 5) for the isotropic ($\Delta T_m^t = 5.8$ K) and fibrillar zones ($\Delta T_m^t = 4.2$ K). The quantity ΔT_m should reflect the dispersion of λ_c. However, from eq. (2), the presence of commensurable amounts of lamellae with different thickness will not yield ΔT_m^t with the observed magnitude. Furthermore, samples showing a narrow range of λ_c dispersion showed a broad melting peak which cannot be explained by only this cause.[34] The explanation of this phenomenon is that there is a second physical cause of the appreciable width of ΔT_m^t, which is apparent even when λ_c is constant; this broadening is due to the cooperative nature of the melting event and, in spite of its higher contribution, is usually overlooked.

According to Wunderlich,[37] melting of a polymer crystal begins in its side face from a defect site (end

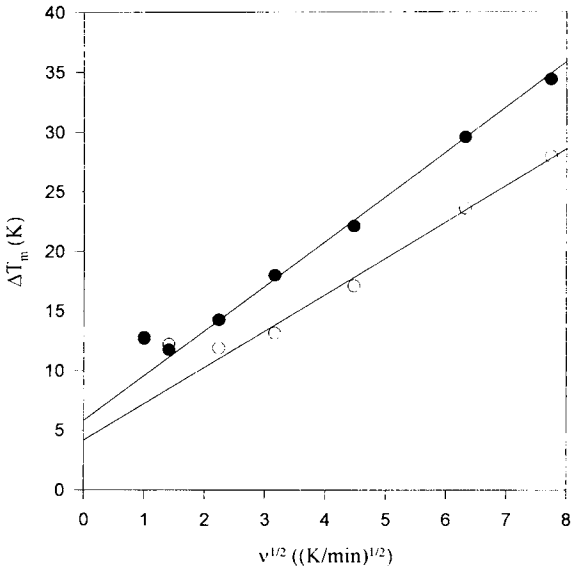

Figure 5 Melting ranges of (●) isotropic and (○) fibrillar zones of iPP deformed samples vs. heating rate.

of chain, fold, etc.) and occurs by the consecutive separation of sections of chains in a direction at right angles to their direction in the crystal. The minimal sequence of repeat units passing as an integral whole from an ordered structure into a disordered state corresponds with an event ("kinetic unit") of a phase transition of an order–disorder kind, i.e., to parameter ν of the intrachain cooperativity of the process.

Initially, the theory of order–disorder phase transitions with determination of parameter ν was developed in connection with the thermodynamics of the helix–random coil transition in proteins.[38] The simultaneous surmounting of barriers to intermolecular interaction, restricting the motion of a chain section and consisting of ν monomer units, was considered, to give, according to Flory,[38] the relation

$$\Delta T_m^t = \frac{2RT^2\sigma_i^{1/2}}{\Delta H} \tag{3}$$

Here, ΔT_m^t is the width of the phase-transition temperature range; T, the average temperature; ΔH, the change in the enthalpy in the transition for a single repeat unit, and σ_i, the characteristic of the cooperativity of the event.

Frenkel[39] postulated that the number of repeat units in the sequence being considered (when $\sigma_i \ll 1$) is $\nu \approx \sigma_i^{-1/2}$, and for the experimental determination of ν, one must measure the temperature dependence of the structure-sensitive property in the region of the order–disorder phase transition. This is why it is possible, by determining the relation $C_p = f(T)$, i.e., on the basis of a DSC curve, to find ν from the equation

$$\nu = \frac{2R(T_m^t)^2}{\Delta T_m^t \Delta H} \tag{4}$$

where $\Delta H \approx \Delta H_m^0$.

The values of ν, calculated from eq. (4), are 15.4 nm for the isotropic region and 21.0 nm for the fibrillar. A first fact deserves commentary: In the isotropic region, the value of ν is of the same order as the one obtained for λ_c. That would indicate that a melting event involves all the repetitive units of a chain fold on the lamellae lateral surface. That result is consistent with other bibliographic data.[34] However, the values of ν for the oriented zone seem to be contradictory because parameter ν increases in this zone to values clearly above λ_c. In the former explanation, which would indicate that the melting event involves more monomer units than those which exist in the actual length of a chain fold on the crystallites. However, this apparent contradiction has a satisfactory explanation which deals with the particular structure of oriented semicrystalline polymers.

An interesting effect has been discovered in HDPE samples in which the disordered component was removed by etching.[34] Here, the melting peak splits and can be divided into two peaks corresponding to values of $\Delta T_{m1}^t \approx 3$ K and $\Delta T_{m2} \approx 1.5$ K. For the first of these, parameter $\nu_1 \approx 20$ nm was close to the X-ray thickness λ_c, while for the second one, it was $(L + \lambda_c) \approx 56$ nm, where L is the long spacing. Then, the values of ν higher than λ_c reveal the existence of "double-folds," i.e., straightened sections of chains extending through two lamellae and including a transection between them. The presence of that second component in the endothermic melting peak indicates that the double folds are arranged not randomly, but form fibril-like structures joining two lamellae. These molecules are also called in the bibliography "taut tie molecules" and their existence has been proved by transmission electron microscopy (TEM)[40,41] and one-dimensional X-ray diffraction.[42] Then, in view of the former explanation, the increase of ν in the oriented portion at values clearly above the lamellar thickness must be interpreted, in our work, as the contribution to the melting process of a certain amount of such molecules, which number increases as the parameter ν augments. In this sense, DSC represents an additional alternative to those methods when one is interested in detecting these molecules in a polymer system.

Finally, the polymer studied can be present under two different crystalline structures, namely, α (predominant in samples obtained from the melt) and β. Those structures have slightly different melting behavior and changes in their relative content will modify the DSC curves. However, both can be distinguished by wide-angle X-ray diffraction and analysis of samples from the isotropic and fibrillar zones reveals a very low and constant content of the β phase (result not shown). Thus, this phenomenon cannot be the cause of artifacts in this study.

Study of the Transition Front

A portion of the polymer similar to the one used in SEM was used for the study of the transition front. This piece was then sliced by a microtome into 100 μm-thick slices. The plane of the slices was perpen-

dicular to the stretching direction (sample axis). In this way, a study of the evolution of the structure can be done from the calorimetric results.

However, a quantitative analysis cannot be properly made, because to obtain the true melting points and range, one must use a high number of equivalent samples which, obviously, is not possible when the transition front is studied. On this point only, experimental values will be used, and to avoid excessive influence of the experimental conditions, a heating rate of 10 K min^{-1} was chosen. It is of crucial importance to avoid the existence of modification of the polymer structure by thermal annealing during the measurement, and when this condition is achieved, thermal lag must to be minimum. The chosen heating rate is the compromise solution for our sample (see Figs. 4 and 5).

The evolution of the melting temperature T_m can be seen in Figure 6. Since according to eq. (1) the relationship between λ_c' and T_m is of the kind

$$\lambda_c' = \frac{1}{a - bT_m} \tag{5}$$

the decrease of T_m, as we move from the isotropic to the fibrillar zone through the transition front, can be interpreted as a decrease of the lateral dimension of the lamellae and the evolution of T_m must be parallel to the evolution of λ_c'. However, although the thermal lag has been minimized as much as possible, this is still high enough to produce unreasonable values of λ_c' from eq. (1). Thus, from this point of view, the evolution of T_m observed in Figure 6 must be understood as, at least, a qualitative picture of λ_c'.

A sigmoidal trend of λ_c' can be proposed; in the isotropic zone and up to the position around +2 mm, no significant changes of the T_m have been found. This indicates that up to this position the integrity of the lamella is essentially preserved. At the first points of the transition front, T_m starts to diminish, which represents the beginning of the chain unfolding in the original lamellae. This fragmentation increases in magnitude as we move to the fibrillar region. At the end of the transition front, the maximum fragmentation was achieved and the original lamella was transformed to a set of microfibrils. Beyond the transition front, in the fibrillar region, no further changes in the microfibrils dimensions was observed.

Finally, the sigmoidal evolution presented here must not be interpreted as a continuous evolution of λ_c'. As shown in Figure 2, in the transition front

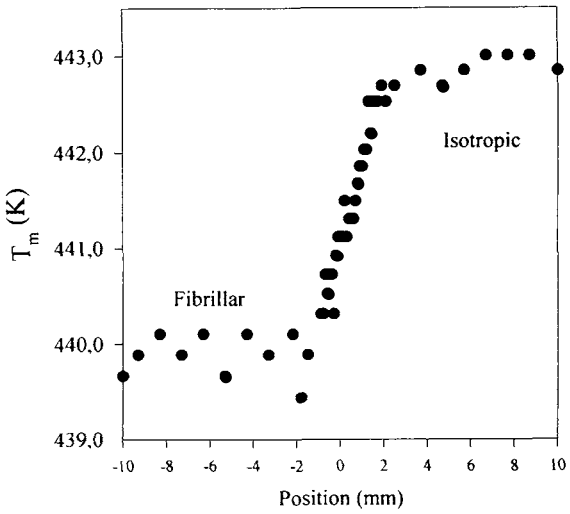

Figure 6 Evolution of the melting peak in the stretched iPP sample. Zero position on the X-axis was estimated as the middle point of the transition front.

coexist fibrillar structures, newly formed inside the cracks, and remains of the original spherullitic. Then, the transition front must be viewed as an inhomogeneous mixture of two different structures: the fibrillar, in which the lamellar fragmentation has been produced practically to its maximum extent, and the spherullitic structure, which will retain the lamellar structure practically intact. The evolution of λ_c' then reflects the increasing of the fraction of material incorporated in fibrillar structures at the expenses of spherullitic material. Due to the global data supplied by the DSC method, the values must be interpreted in terms of the average of an inhomogeneous mixture of both structures in the transition front.

With regard to the parameter of intrachain melting cooperativity, the values of T_m and ΔT_m obtained at 10 K min^{-1}, by using eq. (4), yield the evolution of ν showed in Figure 7. Again, the thermal lag impedes the quantitative analysis and the numerical values of ν are too low compared to those obtained before when T_m^t and ΔT_m^t were used. In any case, and according to the previous discussion, the trend of the curve must be understood as a qualitative picture of the presence of tie molecules and its evolution along the transition front. In this sense, the tie molecules are absent in the isotropic region where the true value of ν is comparable to λ_c. As the observation zone falls in the transition front, ν increases, revealing the presence of initial amounts of tie molecules. The number of them augment as the observation shifts to the oriented zone and, at the extreme of the transition front, reaches a stable value.

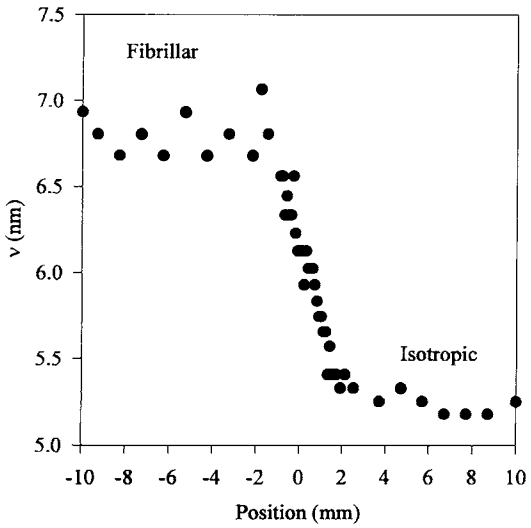

Figure 7 Evolution of the parameter of intrachain melting cooperativity. *X*-axis as in Figure 6.

Finally, the increasing of v as the observation point moves to the oriented zone again has to be interpreted as the result of the average of the presence of taut tie molecules in the fibrillar structures and their absence in the isotropic rest of the spherullites.

CONCLUSIONS

The uniaxially stretching of semicrystalline samples such as the iPP studied here promotes deep changes in the original structure. SEM micrographs showed that the plastic deformation of the spherullites is restricted to the domain of the transition front. The beginning of that deformation of the spherullites, with changes to elipsoidal geometry, coincides with the presence of cracks. In the transition front, an inhomogeneous mixture of newly formed fibrillar material and remains of the original spherullitic (isotropic) structure exists. The fibrillar material appears inside cracks which grow in the transverse direction to the stress direction.

The evolution of the melting temperature along the transition front reveals a qualitative view of the process of lamellae fragmentation. From those data, that fragmentation is mainly restricted to the transition front.

Finally, a significative change in the parameter v has also been found. As happened with other properties observed, changes in v are limited to the transition front. The evolution of this parameter has been associated to the formation of double folds; totally extended chains connecting two neighbor crystallites also called "taut tie molecules." In this sense, the birth and evolution of the tie molecules seem to be also restricted to the transition front.

The apparent progressive modification of the microstructure, suggested by the continuous evolution of the different parameters studied here, must not be understood as the existence of intermediate structures, but, rather, as the coexistence of two arrangements, one coming from the remaining spherullitic structure and the other originated in the microfibrillar structures newly formed inside the crazes, as observed by SEM.

This work was funded by the "Comisión Interministerial de Ciencia y Tecnología/CICYT" (Programme MAT 94-0894).

REFERENCES

1. A. Peterlin, *J. Polym. Sci. C*, **9**, 61 (1965).
2. A. Peterlin, *J. Polym. Sci. C*, **15**, 427 (1967).
3. A. Peterlin, *J. Polym. Sci. C*, **18**, 123 (1967).
4. R. S. Stein, *Proc. R.A. Welch Found. Conf. Chem. Res.*, **10**(Polymers), 207 (1967).
5. R. Bonart, *Koll.-Z. Z. Polym.*, **211**, 14 (1966).
6. A. Peterlin, *Man-made Fibers*, H. F. Mark, S. M. Atlas, and E. Cernia, Eds., Wiley-Interscience, New York, 1967, Vol. 1, pp. 283–340.
7. A. Peterlin, *Koll.-Z. Z. Polym.*, **216–217**, 129 (1969).
8. A. Peterlin, *Polym. Eng. Sci.*, **9**, 172 (1969).
9. E. W. Fischer and M. Goddar, *J. Polym. Sci. C*, **16**, 4405 (1969).
10. R. S. Stein, *Polym. Eng. Sci.*, **9**, 320 (1969).
11. A. Peterlin, *J. Mater. Sci.*, **6**, 490 (1971).
12. K. Sakaoku and A. Peterlin, *Makromol. Chem.*, **108**, 234 (1967).
13. J. L. Williams and A. Peterlin, *J. Polym. Sci. A*, **2**, 211 (1969).
14. K. Kobayashi, *J. Polym. Sci. A*, **2**, 211 (1975).
15. J. Petermann, W. Kluge, and H. Gleiter, *J. Polym. Sci. Polym. Phys. Ed.*, **17**, 1043 (1979).
16. T. Juska and I. R. Harrison, *Polym. Eng. Rev.*, **2**, 13 (1982).
17. T. Juska and I. R. Harrison, *Polym. Eng. Sci.*, **22**, 766 (1982).
18. R. Popli and L. Mandelkern, *J. Polym. Sci. Polym. Phys. Ed.*, **25**, 441 (1987).
19. A. N. Gent and S. Madan, *J. Polym. Sci. Polym. Phys. Ed.*, **27**, 1529 (1989).
20. T. Liu and I. R. Harrison, *Polymer*, **88**, 233 (1988).
21. B. Heise, H.-G. Kilian, and W. Wulf, *Prog. Colloid Polym. Sci.*, **67**, 143 (1980).

22. J. M. Brady and E. L. Thomas, *Polymer,* **30,** 1615 (1989).
23. J. M. Brady and E. L. Thomas, *J. Mater. Sci.,* **24,** 3311 (1989).
24. W. Glenz and A. Peterlin, *J. Polym. Sci. A-2,* **9,** 1191 (1971).
25. P. J. Hendra, M. A. Taylor, and H. A. Willis, *Polymer,* **26,** 1501 (1985).
26. H. W. Siesler, *Adv. Polym. Sci.,* **65,** 1 (1984).
27. H. W. Siesler, *Makromol. Chem. Macromol. Symp.,* **53,** 89 (1992).
28. T. Jawhari, J. C. Merino, J. C. Rodriguez-Cabello, and J. M. Pastor, *Polym. Commun.,* **33,** 4199 (1992).
29. J. M. Pastor, T. Jawhari, J. C. Merino, and J. Fraile, *Makromol. Chem. Macromol. Symp.,* **72,** 131 (1993).
30. J. C. Rodríguez-Cabello, T. Jawhari, J. C. Merino, and J. M. Pastor, *Polymer,* to appear.
31. M. Aboulfaraj, B. Ulrich, A. Dahoun, and C. G'Sell, *Polymer,* **34**(23), 4817 (1993).
32. T. H. Courtney, *Mechanical Behaviour of Materials,* McGraw-Hill Series in Materials Science and Engineering, McGraw-Hill, New York, 1990.
33. R. T. Dehoff and F. N. Rhines, *Quantitative Microscopy,* McGraw-Hill, New York, 1969, Chap. 7.
34. V. A. Bershtein and V. M. Egorov, *Differential Scanning Calorimetry of Polymers. Physics, Chemistry, Analysis, Technology,* Ellis Horwood, London, 1994.
35. Z. Bartczak and A. Galeski, *Polymer,* **31,** 2027 (1990).
36. G. Natta, P. Corradini, and M. Cesari, *Atti Acad. Naz. Lincei Mem. Classe Sci. Fis. Mat. Nat. Sez.,* **21,** 365 (1965).
37. B. Wunderlich, *Macromol. Phys.,* **1–3** (1973, 1976, 1980).
38. P. Flory, *Proc. R. Soc.,* **49,** 151 (1961).
39. S. Frenkel, in *Entsiklopediya Polimerov (Encyclopaedia of Polymers),* Sov. Entsikl, Moscow, 1974, Vol. 2, pp. 127–129.
40. J. Petermenn, W. Kluge, and H. Gleiter, *J. Polym. Sci. Phys. Ed.,* **17,** 1043 (1979).
41. M. Furuta and K. Kojima, *J. Macromol. Sci. Phys. B,* **25**(3), 349 (1986).
42. V. I. Selikhova, L. A. Ozerina, A. N. Ozerin, and N. F. Bakeev, *Vysokomol. Soed. A,* **28**(2), 342 (1986).

Received June 30, 1995
Accepted November 30, 1995